

Static and Dynamic Analysis of Chemical Reactor using the Finite Element Method

*Jong-Rae Cho**, *Boo-Youn Lee***, *Won-Jin Kim***

Abstract

The dynamic analysis and stress analysis of the Linear Low Density Polyethylene (LLDPE) reactor were carried out by using the finite element method. In the dynamic analysis, modal and harmonic response analyses were performed. In the stress analysis, operating pressure and dead weight, wind and seismic loading and horizontal impact forces due to bubbles bursting in the reactor were considered. For the detailed analysis, three-dimensional modeling were carried out by I-DEAS software and finite element analysis by ANSYS software. Results of the analyses satisfy the requirement of ASME Boiler & Pressure Vessel Design Code Section VIII Division 2.

Key Words : Linear low density polyethylene reactor, Finite element method, Dynamic analysis, Stress analysis, Cylindrical column.

I. Introduction

The LLDPE reactor dealt with in present research is a tall cylindrical column as shown in Fig. 1. The tall cylindrical process column is supported on a cylindrical shell with support lugs resting on a concrete foundation and firmly fixed to the foundation by anchor bolts embedded in concrete. The shell thickness of column, as computed by the Code formulas, based on the internal pressure alone, is usually not sufficient to withstand the

* 해양해양대학교 기계냉동자동차공학부

** 계명대학교 자동차공학부

combined stresses produced by the operating pressure plus the weight plus the wind or seismic loads plus another process loadings. According to ASME Boiler & Pressure Vessel Design Code Section VIII Division 1, the shell thickness computations are based on the principal stresses. But the stress intensities govern the vessel thickness required by Code Section VIII Division 2^{(1),(2)}.

Detailed stress analysis is performed considering the effects of each loading and combined loading. The results of the analysis were reviewed and compared with the allowable values. The purpose of this paper is the dynamic analysis and stress analysis, by use of the finite element method, of the LLDPE reactor.

2. Design Criteria

The design criteria are based on ASME Boiler & Pressure Vessel Design Code Section VIII Division 2. In addition, the structural design under dynamic loading for the reactor and support system are based on an Engineering Manual, as

- (i) For modal analysis, the lowest vertical natural frequency is to be greater than 10.8 Hz.

Vibration studies and on-site measurements have shown that reactor/support structure systems with vertical natural frequencies above 9Hz (top end of expected excitation frequency range) have operated without vibration problems. To reduce the possibility of excitation, a safety factor of 1.2 should be applied, and it is therefore recommended that the reactor/support structure system is designed to have a vertical natural frequency in excess of $1.2 \times 9 = 10.8\text{Hz}$.

- (ii) For stress analysis, the reactor and support structure is to be safe under dynamic forces resulting from bubbles bursting in the fluidized bed.

Bubbles in the fluidized bed generate a complex forcing function. The lowest frequencies are below 1Hz, with higher frequencies extending up towards 9Hz. For design purposes the amplitude of the force is estimated to be 100kN in the vertical direction. It is suggested that the total reactor system response is considered for a sinusoidal forcing function, in steps of 1Hz, from 1Hz to 9Hz.

Bubbles bursting against the reactor wall produce a shock loading. Details are imprecise, but for design purposes the value of the impact is estimated to be 2000N.s (equivalent to a mass of 200kg striking the reactor wall at 10m/s). This loading can be considered as acting in any horizontal direction against the reactor wall at the level of the reactor support ring.

3. Procedure of analysis

The geometric modeling of the reactor system was performed by I-DEAS⁽³⁾ Master series version 4.0, solid modeling and analysis program developed and supported by Structural Dynamics Research Co. of Milford, Ohio, U.S.A. The geometric model was transferred to ANSYS⁽⁴⁾ version 5.3, a finite element program by Swanson Analysis Systems Inc of Houston, PA., U.S.A. The reactor system was meshed and analyzed using ANSYS.

The geometric dimensions of the reactor system are as per drawing and supplementary sketches are shown in Fig. 1 and 2. The reactor system is modeled by 4-node and 3-node thin shell elements (SHELL63) and lumped mass elements (MASS21) as shown in Fig. 3 and 4. Number of nodes is 4319 and numbers of SHELL63 elements and MASS21 elements are 4404 and 11, respectively.

Material of the reactor and support structure is SA516-70, and following material properties are used:

$$\text{Young's modulus } E = 21,000 \text{ kg}_f/\text{mm}^2$$

$$\text{Poisson's ratio } \nu = 0.3$$

$$\text{Mass density } \rho = 7.96 \times 10^{-10} \text{ kg}_m/\text{mm}^3$$

In addition to the reactor and support structure, the mass of the fluidized bed, grid and support, internal and external attachment, ladder, insulation, nozzles and manholes are also taken into consideration. For the fluidized bed, the total weight of 71.2ton can be modeled as distributed on the reactor wall, and hence density of the shell elements covering the fluidized bed are appropriately increased considering the weight. For the grid and support, the total weight can be modeled as distributed on the bottom head of the reactor, and hence density of the shell elements of the bottom head are appropriately increased considering their

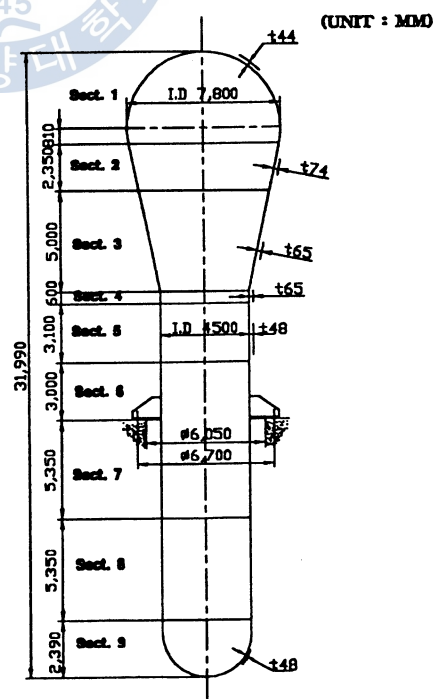


Fig. 1 Schematic sketch of Egypt LLDPE reactor.

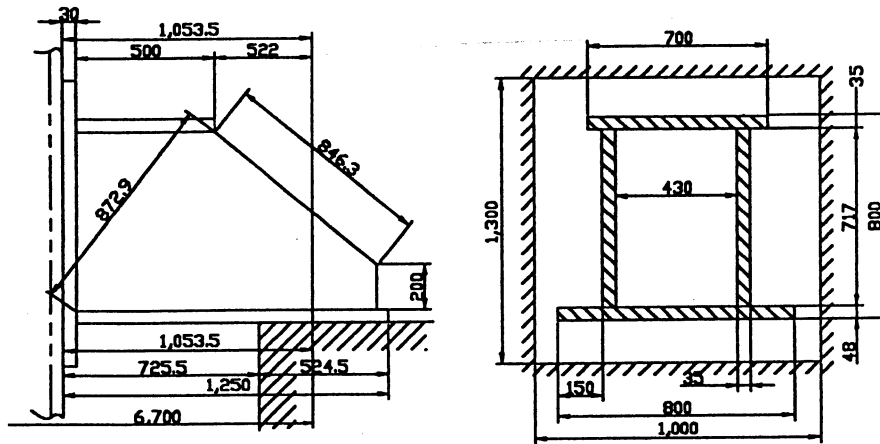


Fig. 2 Dimension of support lug.

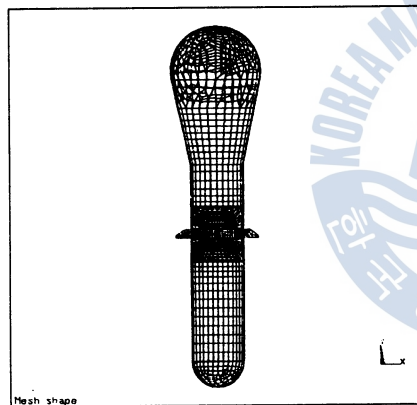


Fig. 3 Finite element model of LLDPE reactor.

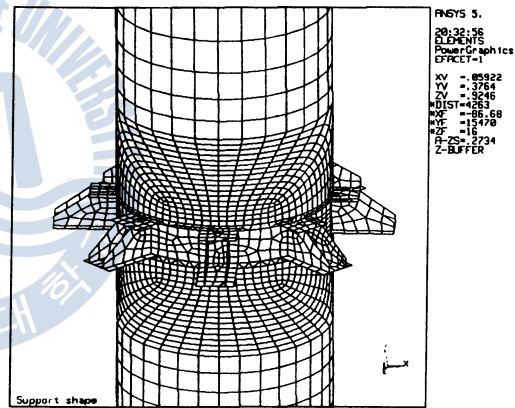


Fig. 4 Finite element model of support lug.

weight. Thus, the density of the shell elements representing the reactor sections in Fig. 1 is determined reflecting the mass of the fluidized bed, grid and support, internal and external attachment, ladder, insulation, and is listed in Table 1.

Table 1 Density of the shell elements of the reactor sections

Section no. in Fig. 1	1	2	3	4	5	6	7	8	9
Density ($10^{-10} \text{kg}_m/\text{mm}^3$)	9.065	8.193	8.120	8.564	10.134	16.860	17.080	17.660	11.030

The nozzles and manholes of which weight are greater than 500kg are modeled by lumped mass elements (MASS21) and relatively lighter ones are ignored.

As shown in Fig. 5 for the boundary conditions, all degrees of freedom are restrained for

the nodes on the anchor bolt position, and vertical displacement is restrained for the nodes on concrete foundation.

For the modal analysis, the subspace iteration method is used and the lowest three normal modes are calculated. In additions, in order to check the possibility of resonance by the vertical dynamic forces from bursting bubbles in the fluidised bed, the harmonic response analysis is performed. The sinusoidal forcing function as specified in Section 2 is used to analyze the response of the reactor. The vertical excitation force having the amplitude of 100kN is equally distributed to the nodes on the reactor wall, of which level is top of the fluidised bed, 14m from the grid location.

For the stress analysis, the operating pressure and dead weight, wind and seismic loading, vertical loading and horizontal impact loading are considered. In case of the operating pressure and dead weight, wind and seismic loading, static analyses are performed for each load case and a combined load case. For the horizontal impact loading, the impact by bubbles bursting against the reactor wall is modeled as a step function and transient dynamic analysis is performed. Amplitude and duration time of the impact are assumed to be 20kN and 0.1sec., respectively. As specified in Section 2, the impact load is radially applied to the wall of the reactor at the level of a support lug position.

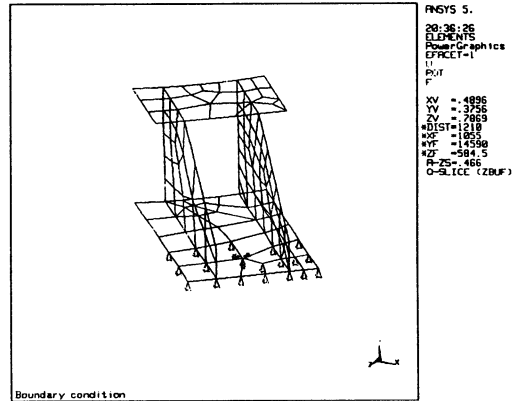


Fig. 5 Boundary condition applied to support lug.

4. Evaluation of analysis results

4.1 Modal analysis and harmonic response analysis

Since the reactor system has an axisymmetric shape, a natural frequency has two same mode shapes so called degenerate modes. Therefore, it is possible to estimate the dynamic characteristics of the system by considering one mode shape for each natural frequency. Three normal modes are calculated by modal analysis and results are summarized in Table 2.

Table 2 Results of modal analysis

Mode no.	1	2	3
Natural frequency (Hz)	4.85	11.45	12.18
Mode shape	Fig. 6	Fig. 7	Fig. 8
Mode description	Rigid rotating mode	Bending mode	Local deformation mode

In the first mode, the reactor rotates horizontally about the support without local deformation with a fundamental natural frequency of 4.85Hz, as shown in Fig. 6. In the second mode, the reactor bends about the support with a natural frequency of 11.45Hz, as shown in Fig. 7. In the third mode, the wall of reactor deforms locally with a natural frequency of 12.18Hz, as shown in Fig. 8. As specified in Section 2, the vertical natural frequency should be greater than 10.8Hz, and this may mislead to a conclusion that the first mode with 4.85Hz violates the design criterion. But we should note that the natural frequency limit is specified in terms of vertical natural frequency. It is caused from the fact that direction of the excitation forces by bursting bubbles in the fluidised bed is in the vertical direction.

Basically, only the mode including a vertical vibration pattern is affected dominantly by the vertical excitation forces. The natural frequency of the first mode is not a vertical natural

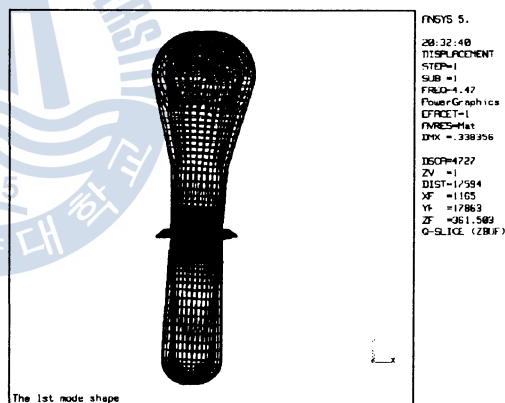


Fig. 6 The 1st mode shape.

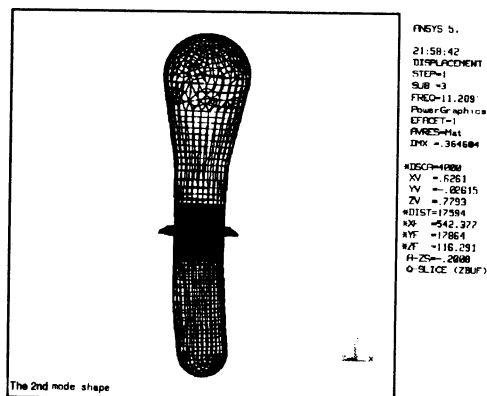


Fig. 7 The 2nd mode shape.

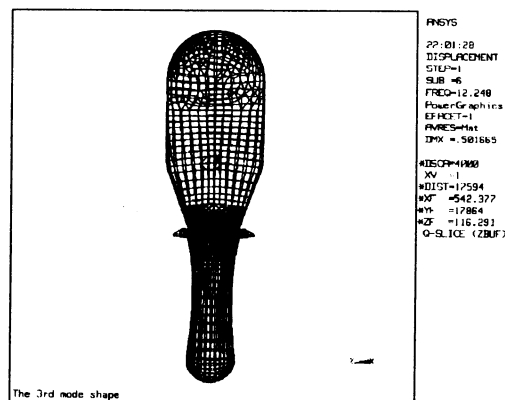


Fig. 8 The 3rd mode shape.

frequency because the first mode is a rigid rotating mode and does not include a vertical vibration pattern. To confirm this problem, it is needed to check the possibility of resonance by the vertical dynamic forces from bursting bubbles in the fluidised bed. For the purpose, the harmonic response analysis is performed. The sinusoidal forcing function in vertical direction as specified in Section 2 is applied, as

$$F_y = 100 \sin(\omega t) \quad (kN)$$

, and response of the reactor system is analyzed. The force is equally distributed to the nodes on the reactor wall, of which level is top of the fluidised bed, 14m from the grid location. The displacement amplitudes versus excitation frequency at an excitation node and

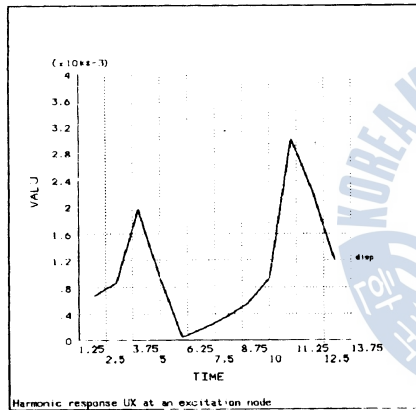


Fig. 9 The displacement amplitude versus excitation frequency at an excitation node. (radial displacement)

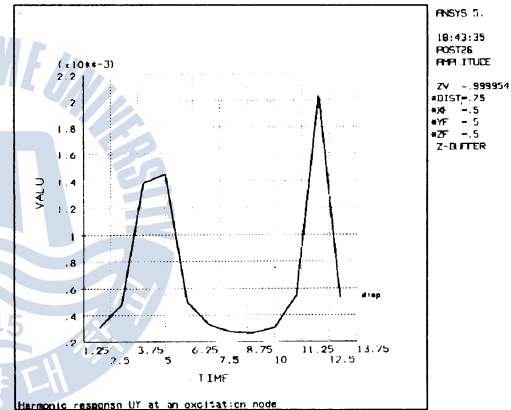


Fig. 10 The displacement amplitude versus excitation frequency at an excitation node. (vertical displacement)

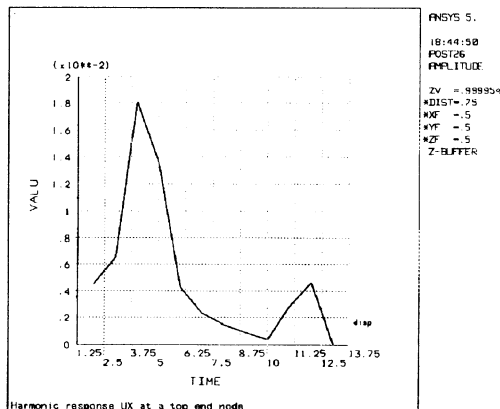


Fig. 11 The displacement amplitude versus excitation frequency at a top end node. (radial displacement)

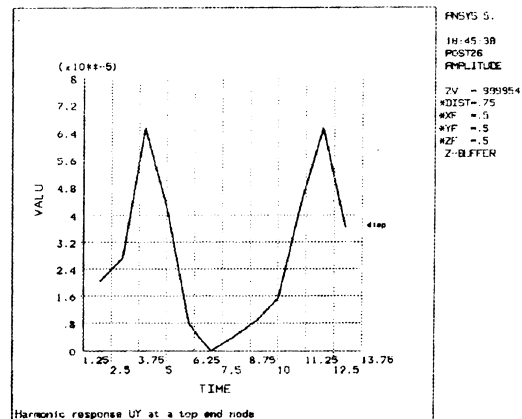


Fig. 12 The displacement amplitude versus excitation frequency at a top end node. (vertical displacement)

a node located on top end of the reactor are shown in Fig. 9-12. Even though the peak of displacement amplitude appears at the first natural frequency as shown in Fig. 10 and 11, the largest displacement occurring at the node on top end of the reactor is a very small value of 0.021mm as shown in Fig. 11. It is confirmed that no vibration problem occurs by the vertical excitation forces with frequencies lower than 10.8Hz, and we can conclude that the vertical natural frequency of the reactor/support structure system meets the design criteria.

4.2 Stress analysis

4.2.1 Static loading

(1) Operating pressure and dead weight

The operating pressure of $0.273\text{kg}_f/\text{mm}^2$ is applied for reactor section from 1 to 8 and $0.3\text{kg}_f/\text{mm}^2$ for section 9. The all dead weights of the reactor system are also applied in the analysis. The deformed shape is shown in Fig. 13 and the maximum displacement is 4.08mm. A contour plot of the stress intensity is shown in Fig. 14. The maximum stress intensity is $14.93\text{kg}_f/\text{mm}^2$ at junction of the top head and the conical shell and is

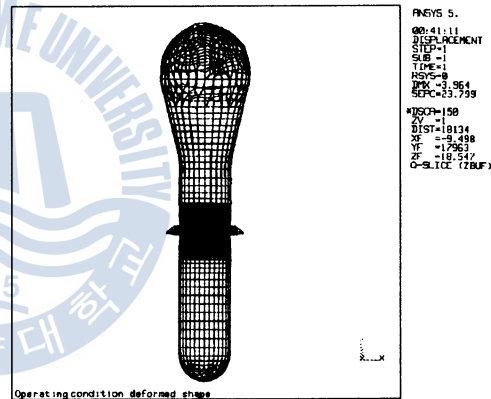


Fig. 13 Deformed shape under operating pressure and dead weight loading.

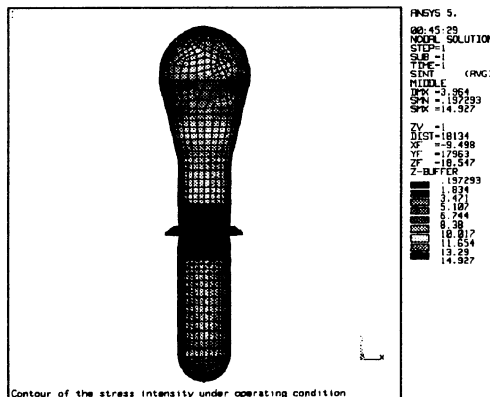


Fig. 14 Contour of the membrane stress intensity under operating pressure and dead weight loading.

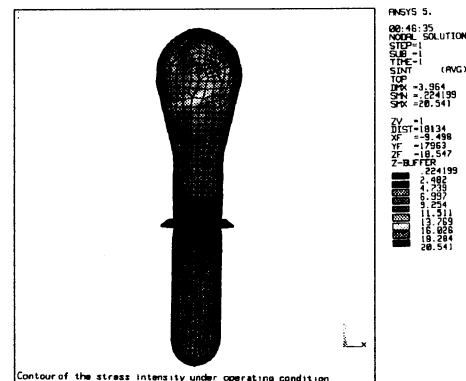


Fig. 15 Contour of the membrane+bending stress intensity under operating pressure and dead weight loading.

less than the allowable value of $15.96\text{kg}_f/\text{mm}^2$. A contour plot of the membrane+bending stress intensity is shown in Fig. 15. The maximum membrane+bending stress intensity is $20.54\text{kg}_f/\text{mm}^2$ and is less than the allowable value of $23.94\text{kg}_f/\text{mm}^2$.

(2) Wind and seismic loading

The design wind pressure (P_w) and wind load (F_w) per UBC Code are expressed as

$$P_w = C_e \times C_q \times q_s \quad (\text{kg}_f/\text{m}^2)$$

$$F_w = P_w \times A \quad (\text{kg}_f)$$

where C_e is exposure factor, C_q shape factor, q_s wind stagnation pressure, and A projected area. The basic wind pressure is 44.5 m/s .

The lateral force due to earthquake load is applied as per UBC.

$$V = \frac{ZIC}{R_w} W$$

where Z : seismic zone factor (zone 3) = 0.3,

I : information factor = 1.0,

C : numerical coefficient = 2.232,

R_w : numerical coefficient = 4,

W : total dead weight.

Because the wind loading and seismic loading are applied in same direction, greater stress occurs under the combined loading than under each loading: wind or seismic loading. Hence, superposition of the two loading results in conservative solution. A contour plot of the membrane stress intensity is shown in Fig. 16. The maximum membrane stress intensity is $3.87\text{kg}_f/\text{mm}^2$ at the support lug.

(3) Combined loading

Combined loading superposes three static load cases: operating pressure and dead weight, wind and seismic loading, and vertical loading. The deformed shape is shown in Fig. 17 and the maximum displacement is 4.21mm . A

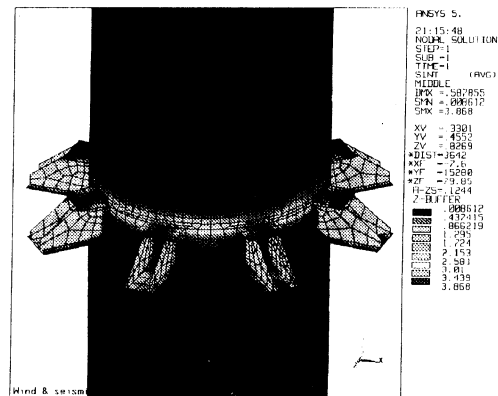


Fig. 16 Contour of the membrane stress intensity under wind and seismic loading.

contour plot of the membrane stress intensity is shown in Fig. 18. The maximum value is 14.94kgf/mm^2 at junction of the top head and the conical shell and is less than the allowable value of 19.15kgf/mm^2 . A contour plot of the membrane+bending stress intensity is shown in Fig. 19. The maximum value is 20.55kgf/mm^2 and is less than the allowable value of 28.73kgf/mm^2 . A contour plot of the minimum principal stress is shown in Fig. 20. The maximum compressive stress of the top plate of the support lug is 11.85kgf/mm^2 . Considering that buckling is to be checked at the wall of reactor, the maximum compressive stress is about 4.3kgf/mm^2 and is less than the allowable value of 12.99kgf/mm^2 .

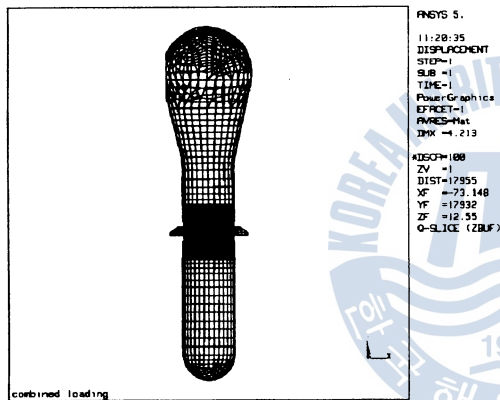


Fig. 17 Deformed shape under combined loading.

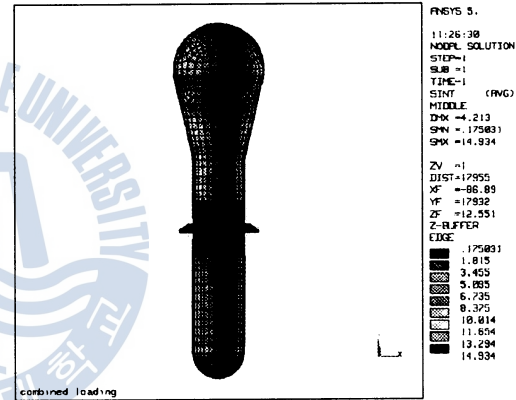


Fig. 18 Contour of the membrane stress intensity under combined loading.

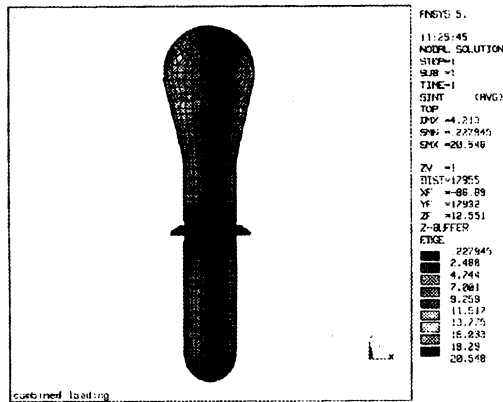


Fig. 19 Contour of the membrane+bending stress intensity under combined loading.

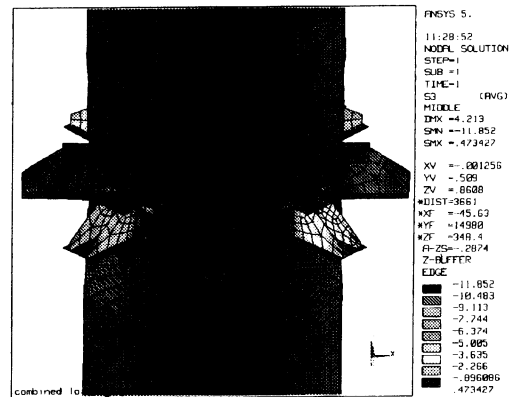


Fig. 20 Contour of the minimum principal stress under combined loading.

4.2.2 Horizontal impact loading

To calculate stresses resulting from the shock loading by bubbles bursting against the reactor wall, the impact load is modeled as a step function and transient dynamic analysis is performed. Amplitude and duration time of the impact is set to be 20kN and 0.1sec., respectively. The force is radially applied to the inner wall of the reactor at the level of a support lug position. Two cases are analyzed depending on the impact points: cases of the impact points A and B as noted in Fig. 21. The points A and B represent the position on the wall where the support lug is attached and not attached, respectively.

For the case of the impact point A, time history of the radial displacement at the impact point is shown in Fig. 22. The maximum displacement is 0.02mm and occurs at 0.02sec.

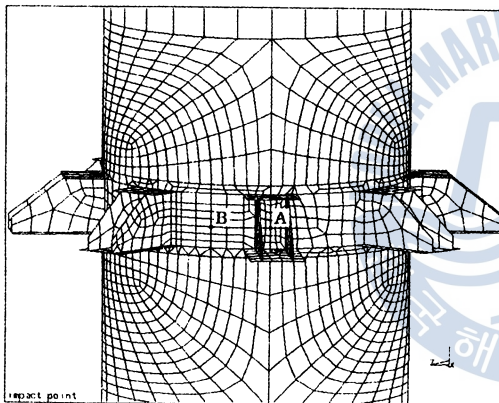


Fig. 21 Two impact points at the level of the reactor support rings.

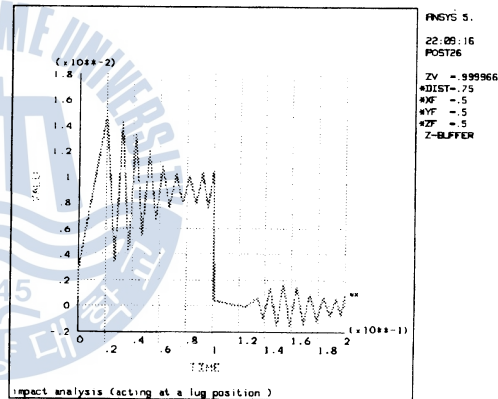


Fig. 22 Time history of radial displacement at the impact point A.

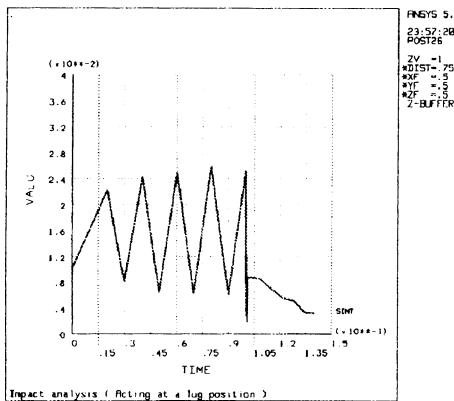


Fig. 23 Time history of the membrane stress intensity at the impact point A.

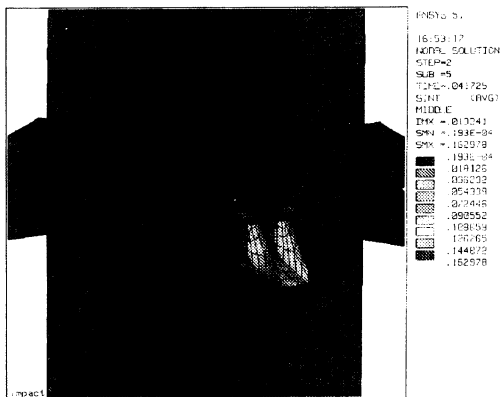


Fig. 24 Contour of the membrane stress intensity under impact loading on point A.

Time history of the membrane stress intensity at the impact point is shown in Fig. 23. The maximum membrane stress intensity is $0.16\text{kgf}/\text{mm}^2$ at a gusset plate and occurs at 0.042sec . A contour plot of the membrane stress intensity at 0.042sec is shown in Fig. 24. The maximum membrane+bending stress intensity is $0.33\text{kgf}/\text{mm}^2$.

For the case of the impact point B, time history of the radial displacement at the impact point is shown in Fig. 25. The maximum displacement is 0.06mm and occurs at 0.02sec . Time history of the membrane stress intensity at the impact point is shown in Fig. 26. The maximum membrane stress intensity is $0.36\text{kgf}/\text{mm}^2$ at a base plate and occurs at 0.02sec .

As shown in Fig. 24, the horizontal impact loading affects only a local region about the impact point and resulting stresses are negligibly small.

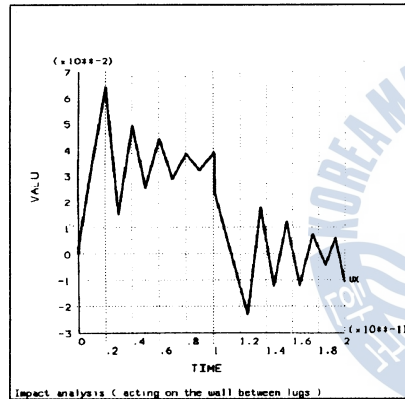


Fig. 25 Time history of radial displacement at the impact point B.

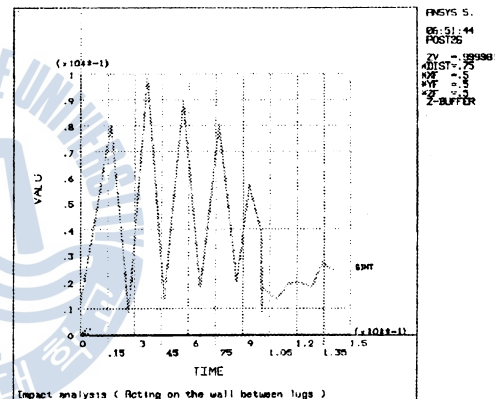


Fig. 26 Deformed shape under impact loading on point B.

5. Conclusions

Summarizing the results of modal analysis and harmonic response analysis, the vertical natural frequency is greater than the lower limit, 10.8Hz , meeting the design criteria. For results of stress analysis under operating pressure and dead weight, wind and seismic loading and horizontal impact forces as summarized in Table 3, the maximum membrane and membrane+bending stress intensity are less than the design stress intensity and the maximum compressive stress is less than the allowable compressive stress. Therefore, this reactor satisfies the requirement of ASME Boiler & Pressure Vessel Design Code Section VIII Division 2 and Engineering Manual.

A method of the three-dimensional finite element modeling and analysis is presented in this paper, and it can be applied in design stages of similar chemical reactors.

Table 3. Summary of results of stress analysis (unit: kg/mm^2)

		Load case	
		Operating pressure and dead weight	Operating pressure and dead weight, wind and seismic, and dynamic loading
Membrane SI	Maximum SI	14.93	14.93
	Design SI	$S_m=15.96$	$1.2S_m=19.15$
Membrane+ bending SI	Maximum SI	20.54	20.55
	Design SI	$1.5S_m=23.94$	$1.2 \times 1.5S_m=28.73$
Buckling	Maximum compressive stress	-	4.3
	Allowable compressive stress	-	$S_c=12.99$

Note) SI: Stress Intensity

References

1. Henry H. Bednar, Pressure vessel design handbook, Van Nostrand Reinhold Company, 1981.
2. ASME Boiler & Pressure Vessel Design Code Section VIII Division 2, ASME, 1995.
3. I-DEAS Master series, Exploring I-DEAS Design, Structural Dynamics Research Corporation, 1998.
4. ANSYS users manual, Swanson Analysis System Inc.

